



ELSEVIER

Available online at www.sciencedirect.com

SCIENCE @ DIRECT®

Physics Letters A 316 (2003) 311–316

PHYSICS LETTERS A

www.elsevier.com/locate/pla

Dependence of the spiral rotation frequency on the surface curvature of reaction–diffusion systems

Niklas Manz^{a,b,*}, V.A. Davydov^c, Stefan C. Müller^b, Markus Bär^a

^a *Max-Planck-Institut für Physik komplexer Systeme, Nöthnitzer Straße 38, D-01187 Dresden, Germany*

^b *Institut für Experimentelle Physik, Otto-von-Guericke-Universität, D-39106 Magdeburg, Germany*

^c *Moscow State Institute of Radioengineering, Electronics and Automation, Vernadsky Prospect 78, 117454 Moscow, Russia*

Received 15 May 2003; accepted 16 July 2003

Communicated by C.R. Doering

Abstract

The dynamic behaviour of spiral waves rotating on surfaces of curved reaction–diffusion systems depends strongly on the curvature of the surface. It was shown in an earlier experiment that a spiral in a Belousov–Zhabotinsky system on a paraboloid drifts to the point of highest Gaussian curvature, as predicted numerically and analytically. Beyond this, theoretical work predicts an increase of the rotation frequency of spiral waves with an increase in the curvature of the system surface (e.g., spirals on different spherical surfaces with decreasing radii). This behaviour leads to an additional term in the function for the rotation frequency proportional to the Gaussian curvature of the system. In this Letter we combine both effects to determine the curvature dependence of the spiral rotation frequency in curved reaction–diffusion systems. On a non-homogeneously curved surface, the spiral tip (the inner end of a spiral) drifts through regions with increasing surface curvature. Measurements of the rotation frequency performed during this propagation verify the predicted effect. The experimental data are confirmed by analytical results in the framework of the kinematic theory.

© 2003 Elsevier B.V. All rights reserved.

PACS: 05.45.-a; 05.70.Ln; 82.40.Ck

Keywords: Belousov–Zhabotinsky reaction; Curved surfaces; Excitation waves; Nonlinear dynamics

Excitation waves occur in different fields related to nonlinear dynamics. These waves can be observed in many biological, chemical, and physical systems [1–3]. A laboratory model of these reaction–diffusion (RD) waves, the Belousov–Zhabotinsky (BZ) reaction [4], has been investigated in one-, two-, and three-

dimensional geometries. So far, most of the theoretical and experimental studies of two-dimensional excitable systems, which are pertinent to this work, have dealt with planar geometries. But in nature many excitable reactions occur on curved surfaces such as the chicken retina [5], the heart muscle [6], and the cortex [7]. In all non-planar media the geometry has an influence on the dynamics of propagating planar fronts or spiral waves [8] and has to be considered in uniformly curved surfaces (e.g., spheres and cylindrical surfaces) as well as non-uniformly curved surfaces

* Corresponding author. Present address: Department of Chemistry and Biochemistry, Florida State University, Tallahassee, FL 32306-4390, USA.

E-mail address: nmanz@chem.fsu.edu (N. Manz).

(e.g., paraboloid and ellipsoid). On spherical surfaces with different radii the rotation frequency of spirals depends on the curvature of the system [9,10]. On an ellipsoid of revolution, for example, such a wave drifts to the point of highest Gaussian curvature [11,12].

In this Letter we use the experimentally shown spiral drift [13] to verify the predicted dependence of the spiral rotation frequency on the surface curvature of the reaction–diffusion system.

Excitable media can be described by a set of nonlinear reaction–diffusion equations. In the simplest case only two variables are used [14]. On curved surfaces the equations for a two-variable system can be written in the following form

$$\begin{aligned}\frac{\partial u}{\partial t} &= F_1(u, v) + D_u \frac{1}{\sqrt{g}} \frac{\partial}{\partial x^i} \left(g^{ik} \sqrt{g} \frac{\partial u}{\partial x^k} \right), \\ \frac{\partial v}{\partial t} &= \epsilon F_2(u, v) + D_v \frac{1}{\sqrt{g}} \frac{\partial}{\partial x^i} \left(g^{ik} \sqrt{g} \frac{\partial v}{\partial x^k} \right),\end{aligned}\quad (1)$$

where u and v are the activator and inhibitor variables, respectively. D_u and D_v are their diffusion coefficients. The nonlinear functions F_1 and F_2 specify the reactions in the system. x^k are the coordinates on the surface and g is the determinant of the metric tensor g_{ik} .

In this model the null isoclines $F_1(u, v) = 0$ and $F_2(u, v) = 0$ have an inverse N -shaped form and a monotonic increasing function, respectively. Usually the analytical study of excitation wave structures described by the “microscopic” equations (1) is impossible. One has to apply numerical simulations or approximate phenomenological methods.

We will use the so-called “kinematic approach” [15,16]. The effectiveness of the kinematic theory is confirmed by a large number of predictions and explanations of effects concerned with the propagation of excitation waves in isotropic, anisotropic, non-stationary, and non-homogeneous excitable media. In the framework of the kinematic theory, an excitation wave is completely determined by specifying the line of its front. The shape and evolution of the wave front can be described by its natural equation $k_g = k_g(l, t)$, where k_g defines the geodesic curvature by its arclength l and time t . Each section of the front moves in the normal direction with the velocity $V = V_0 - D_u k_g$, where the parameter V_0 denotes the velocity of the front with zero geodesic curvature and D_u is

the diffusion coefficient of the activator. The free end of a broken front (tip) can grow or contract with a tangential velocity $c = \gamma(k^* - k_{g0})$, where k_{g0} and k^* are the geodesic curvature of the front near the tip and the critical curvature of the broken front, respectively. The coefficient γ satisfies $\gamma \sim D_u - D_v$. Note that in excitable media with equal diffusion coefficients of the activator and inhibitor $\gamma = 0$ and in jelled BZ systems with an immobilized catalyst $\gamma = D_u$. The main kinematic equation for the evolution of the front on curved surface has the following form [11]:

$$\frac{\partial k_g}{\partial t} \left(\int_0^l k_g V d\xi + c \right) + \frac{\partial k_g}{\partial t} + \frac{\partial^2 V}{\partial l^2} + k_g^2 V = -\Gamma V,$$

where Γ is the Gaussian curvature of the surface. As shown in [11], a spiral wave on the spherical surface rotates faster than on the plane and the additional term is proportional to Γ :

$$\omega = \omega_0 \left(1 + \frac{V_0 \Gamma}{2\xi^2 D_u k^{*3}} \right).\quad (2)$$

Here $\xi = 0.685$ and ω_0 and ω denote the angular velocities of a spiral wave on a plane and on a curved surface, respectively. The expression (2) is valid if the radius of the sphere is much larger than the radius of the spiral wave core. In the case of a small sphere the angular velocity is proportional to $\sqrt{\Gamma}$ [12].

The instantaneous angular velocity of the spiral wave rotating on the non-uniformly curved surface will change in time approximately periodically. These variations of ω will result in a slow drift of the spiral wave core.

In the simplest case of a non-uniformly curved surface of revolution, its Gaussian curvature can be considered as a function of the polar angle, i.e.: $\Gamma = \Gamma(\theta)$. The drift of spiral waves on such surfaces was studied numerically and analytically in the framework of the kinematic approach [13]. The following expressions for angular velocities of the drift were obtained:

$$\frac{d\theta_0}{dt} = \frac{\gamma k^* r_0}{4} \frac{d\Gamma}{d\theta} \quad \text{and} \quad (3)$$

$$\frac{d\varphi_0}{dt} = \frac{V_0 r_0}{4 \sin \theta_0} \frac{d\Gamma}{d\theta}, \quad (4)$$

where θ_0 and φ_0 are the polar and azimuth coordinates of the spiral wave core, respectively; r_0 is its radius. As follows from Eqs. (3) and (4) the theory predicts the

velocities of the drift to be proportional to the gradient of the Gaussian curvature. For a paraboloid or a prolate ellipsoid of revolution, $d\Gamma/d\theta < 0$. Thus, the spiral wave will climb up to the “top” of the paraboloid or prolate ellipsoid with a velocity proportional to $\gamma \sim D_u - D_v$. The velocity of the motion perpendicular to the gradient of the Gaussian curvature (along equi-curvature contour lines) does not depend directly on γ . The trajectory of the core center will have a spiral-like shape. In the particular case of equal diffusivities the spiral wave will drift along the equi-curvature line of a paraboloid or ellipsoid. This case was considered in [9].

The drift of spiral waves described above was shown experimentally [13]. In that experiment the parabolic surface, made of mesoporous glass, was used as a BZ reaction medium. During the experiments the drift towards the top of the paraboloid was observed and the measured velocities were in good qualitative agreement with the kinematic theory.

We use these results to verify experimentally the theoretical prediction that the rotation frequency increases with an increase in surface curvature in a quasi-two-dimensional system. Instead of high-precision measurements of spiral tip positions at sites below the peak in this highly curved system we determine the spiral rotation frequency in a planar part of the reaction medium. Consider at first a paraboloid of revolution specified by the Cartesian equation $z = p(x^2 + y^2)$ with a parameter $p > 0$ and the Cartesian coordinates x and y . The Gaussian curvature of this paraboloid is given by $\Gamma = (4A^2)/(1 + 4A^2r^2)^2$, where A denotes the amplitude at a radius r . Near the top of a paraboloid its Gaussian curvature can be written as

$$\Gamma = \frac{4A^2}{(1 + \theta^2)} \approx 4A^2(1 - 2\theta^2), \quad (5)$$

where θ is the polar angle measured with respect to the z -axis.

Note that not only paraboloids, but also many other surfaces, have Gaussian curvature near the top, described by Eq. (5). As an important example we consider the surface

$$z(x, y) = B \cos^2(bx) \cos^2(by), \quad (6)$$

with the amplitude B , the cartesian coordinates x and y defined by $(-\pi/2b \leq x, y \leq \pi/2b)$, and the wave number b with the wavelength λ defined by

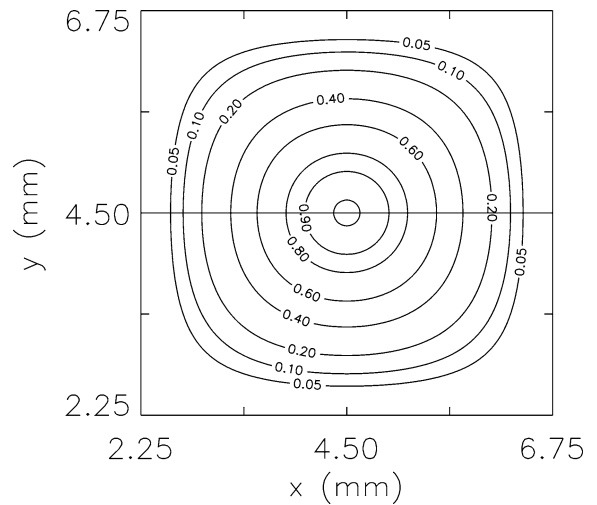


Fig. 1. Contour plot of a maximum of the surface defined by Eq. (6) with an amplitude $B = 1.0$ mm and a wavelength $\lambda = 9.0$ mm.

$b = 2\pi/\lambda$. As one can see in Fig. 1 the top of the extrema of this surface has a parabolic shape according to $A = Bb^2/2$ and can be described by the equation $z = A(1 - b^2r^2/2)$.

The spiral wave, which is slowly climbing to the top of the paraboloid, will successively pass through regions with increasing Gaussian curvature. Therefore, its instantaneous angular velocity ω will also increase according to Eq. (2).

One has to find the function $\omega(t)$. Substitution of Eq. (5) into Eq. (3) leads to the following equation:

$$\frac{d\theta_0}{dt} = -4A^2\gamma k^* r_0 \theta_0.$$

Its solution is

$$\theta_0 = \Theta_0 e^{(-4A^2\gamma k^* r_0 t)}, \quad (7)$$

where Θ_0 is the polar angle determining the initial position of the core. This value also includes the wavelength λ of surfaces similar to Eq. (6). Substituting Eq. (5) into Eq. (2), taking into account Eq. (7) and the fact that we used a BZ system with an immobilized catalyst ($D_v = 0 \rightarrow \gamma = D_u$), we finally obtain the sought-for dependence $\omega(t)$:

$$\omega(t) = L - M \cdot e^{-\beta t}, \quad (8)$$

with the parameters

$$L = \omega_0 \left(1 + \frac{2A^2 V_0}{\xi^2 D_u k^* 3} \right),$$

$$M = \frac{4A^2 V_0 \omega_0 \Theta_0^2}{\xi^2 D_u k^* r_0^3}, \quad \text{and}$$

$$\beta = 8A^2 D_u k^* r_0.$$

As mentioned above the exponential time-dependence found for the angular velocity of the spiral wave (Eq. (8)) is valid not only for a paraboloid but for a wide class of non-uniformly curved surfaces with one or several maxima of the Gaussian curvature. The experimental observation of this dependence will be an indirect but convincing confirmation of the theoretical predictions (2) and (3).

The experimental results were obtained by using a new method for the fabrication of quasi two-dimensional, non-homogeneously curved BZ systems [17,18]. For this experiment, an acrylic glass mould was produced. This mould has two complementary surfaces with a constant distance of 0.30 mm in normal direction at each point [19]. After closing the system, one obtains a planar region of $(75 \times 75) \text{ mm}^2$ which includes 13 spatially distributed hills defined by

$$z(x, y) = B \cos^2(bx) \cos^2(by),$$

$$(-\pi/2b \leq x, y \leq \pi/2b), \quad (9)$$

with amplitudes B of 1 mm or 2 mm and wavelengths $\lambda = b/(2\pi)$ between 4 mm and 10 mm. Each hill has a different combination of these two parameters.

For the experiments we filled the mould with a BZ reaction layer embedded in a silica gel. Ferroin, the redox catalyst normally used for investigating BZ waves, was replaced by the tris(2,2'-bipyridine)ruthenium(II) complex $(\text{Ru}(\text{bpy})_3^{2+})$ [20]. Illuminating the catalyst produces a photochemically excited state, which then catalyzes the production of the inhibitor species Br^- [21]. This effect was used to create spirals at defined positions: When a propagating excitation front reached the requested position, we illuminated one part of the wave from this position to the layer boundary with white light (Zeiss KL 1500 LCD) and obtained one open wave end [22]. This created the spiral tip and finally a spiral wave. One example of such a spiral is shown in Fig. 2.

To avoid hydrodynamic perturbations and, more important, to facilitate the realization of the curved BZ system, the catalyst $\text{Ru}(\text{bpy})_3^{2+}$ was immobilized in a silica gel matrix (Fluka) [23]. Beyond this, the immobilization is a necessary condition for the spiral drift. After filling the negative curved parts of the hills

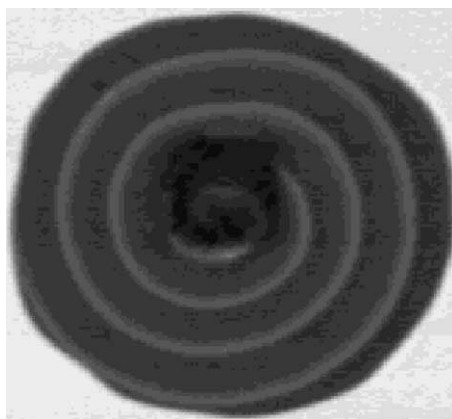


Fig. 2. Total view of a nearly circular reaction system with a spiral wave on the side of a hill with $B = 1.0 \text{ mm}$ and $\lambda = 10.0 \text{ mm}$ defined by Eq. (9). The darker region in the center with a quadratic surface area corresponds to a hill as shown in Fig. 1. Initial concentrations: 358 mM H_2SO_4 , 167 mM malonic acid, 90 mM NaBr , 198 mM NaBrO_3 , and 4.20 mM $\text{Ru}(\text{bpy})_3^{2+}$. Field of view: $(20 \times 19) \text{ mm}^2$.

with 0.1 ml of the liquid gel, we closed the mould. About 5 min later we separated the acrylic glass plates to obtain the non-uniformly curved BZ system with a surrounding, nearly circular planar region as shown in Fig. 2. This gel was neutralized for 30 min with 0.1 M H_2SO_4 and then washed twice for 15 min with distilled water.

The stock solutions of 2.0 M NaBr , 2.0 M NaBrO_3 , and 4.0 M malonic acid (all from Riedel–de Häen) were prepared in distilled water. The catalyst $\text{Ru}(\text{bpy})_3^{2+}$ (20.5 mM, Johnson Matthey) was prepared in 25 mM H_2SO_4 . No further treatment was applied to H_2SO_4 (5 M, Roth).

The two-dimensional transmission of blue light, generated with a light source (Schott–Fostec DCR III) and an $(8'' \times 8'')$ Fostec backlight through the system was detected with a monochrome charge-coupled-device camera (Hitachi KP-M1 CCIR, 758 pixel \times 576 pixel). Single frames were digitized online with a rate of $1.0 \text{ frames s}^{-1}$ using an image-acquisition card (Data-Translation DT3155). The digital data were analyzed later on a personal computer.

When the phase equilibrium between the liquid and the gel had been practically established, and disregarding the slow bromination of malonic acid, the initial concentrations in the gel matrix in this particular experiment were calculated as follows: 358 mM

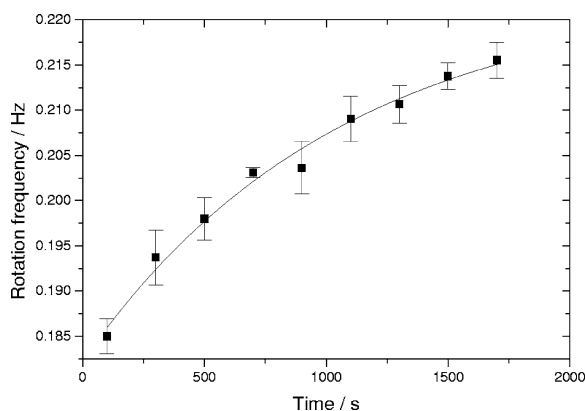


Fig. 3. Evolution of the rotation frequency of the spiral shown in Fig. 2. The experimental data (■) were measured in the planar part of the system. The line shows the fit according to Eq. (8) with the fit parameter $L = 223$ mHz, $M = 40.1$ mHz, and $\beta = 9.48 \times 10^{-3} \text{ s}^{-1}$.

H_2SO_4 , 167 mM malonic acid, 90 mM NaBr, 198 mM NaBrO_3 , and 4.20 mM $\text{Ru}(\text{bpy})_3^{2+}$.

As described above, the tip of a spiral wave on a non-uniformly curved BZ system drifts to the point of highest Gaussian curvature. If the spiral rotation frequency depends on the curvature of the system as predicted in Refs. [11,12] the frequency should increase during the drift. We therefore created spiral waves at the side of a hill and measured the rotation frequency of the spiral in the planar part. Fig. 3 shows the result for the experiment shown in Fig. 2 and represents experiments on hills with other combination of amplitude B and wavelength λ . One can see that the rotation frequency increases as time increases. During this time the spiral drifts to the point of highest Gaussian curvature. Therefore, the rotation frequency is proportional to the spiral drift.

This excellent agreement between the analytically found dependence of the spiral rotation frequency as a function of time (8) and the experiment in Figs. 2 and 3 is also found for other concentrations and on different hills.

In this Letter we present an experimental verification of the dependence of the spiral rotation frequency on the system curvature as predicted theoretically [11, 12]. In [13] it was shown that the spiral tip drifts on a non-uniformly curved BZ system to the point of highest Gaussian curvature. We therefore created quasi-two-dimensional non-uniformly curved BZ media with increasing Gaussian curvature. Rotating spi-

ral waves in this curved system are propagating from lower curved regions to regions with higher Gaussian curvature. This effect is used to verify indirectly the dependence of spiral rotation frequencies on the curvature of the system. In further experiments the method for the fabrication of quasi-two-dimensional, curved BZ systems should be used to produce homogeneously curved reaction media. One then can perform direct measurements of the rotation frequency on surfaces with different Gaussian curvature.

Acknowledgements

N.M. thanks the Max-Planck-Institut für Physik komplexer Systeme and the Deutsche Forschungsgemeinschaft for financial support. V.A.D. was partly supported by the US CRDF-RF Ministry of Education, Grant No. VZ-010-0.

References

- [1] R.J. Field, M. Burger (Eds.), *Oscillations and Traveling Waves in Chemical Systems*, Wiley, New York, 1985.
- [2] A.V. Holden, M. Markus, H.G. Othmer (Eds.), *Nonlinear Wave Processes in Excitable Media*, Plenum, New York, 1991.
- [3] I.R. Epstein, J.A. Pojman, *An Introduction to Nonlinear Chemical Dynamics*, Oxford Univ. Press, Oxford, 1998.
- [4] A.N. Zaikin, A.M. Zhabotinsky, *Nature (London)* 225 (1970) 535.
- [5] N.A. Gorelova, J. Bureš, *J. Neurobiol.* 14 (1983) 353.
- [6] J.M. Davidenko, P. Kent, J. Jalife, *Physica D* 49 (1991) 182.
- [7] V.I. Koroleva, J. Bureš, *Brain Res.* 173 (1979) 209.
- [8] V.S. Zykov, *Simulation of Wave Processes in Excitable Media*, Manchester Univ. Press, Manchester, 1987.
- [9] P.K. Brazhnik, V.A. Davydov, A.S. Mikhailov, *Theor. Math. Phys.* 74 (1988) 300.
- [10] V.S. Zykov, S.C. Müller, *Physica D* 97 (1996) 322.
- [11] A.Yu. Abramychev, V.A. Davydov, V.S. Zykov, *JETP Lett.* 70 (1990) 666.
- [12] V.A. Davydov, V.S. Zykov, *Physica D* 49 (1990) 71.
- [13] V.A. Davydov, V.S. Zykov, T. Yamaguchi, *Macromol. Symp.* 160 (2000) 99.
- [14] J.J. Tyson, P.C. Fife, *J. Phys. Chem.* 73 (1980) 2224.
- [15] V.A. Davydov, V.S. Zykov, A.S. Mikhailov, *Sov. Phys. Usp.* 34 (1991) 665.
- [16] A.S. Mikhailov, V.A. Davydov, V.S. Zykov, *Physica D* 70 (1994) 1.
- [17] V.A. Davydov, N. Manz, O. Steinbock, V.S. Zykov, S.C. Müller, *Phys. Rev. Lett.* 85 (2000) 868.
- [18] N. Manz, S.C. Müller, *Rev. Sci. Instrum.*, accepted for publication.

- [19] N. Manz, Ph.D. Thesis, Otto-von-Guericke-Universität, Magdeburg, 2002.
- [20] V. Gáspár, G. Bazsa, M.T. Beck, *Z. Phys. Chem. (Leipzig)* 264 (1983) 43.
- [21] L. Kuhnert, *Nature (London)* 319 (1986) 393.
- [22] O.-U. Kheowan, V.S. Zykov, S.C. Müller, *Phys. Chem. Chem. Phys.* 4 (2002) 1334.
- [23] T. Yamaguchi, L. Kuhnert, Zs. Nagy-Ungvarai, S.C. Müller, B. Hess, *J. Phys. Chem.* 95 (1991) 5831.